# Inelastic neutron scattering by coupled rotational and translational modes in KCN

**Alois Loidl, K. Knorr, J. Daubert, W. Dultz, W. J. Fitzgerald**

**Angaben zur Veröffentlichung / Publication details:**

Loidl, Alois, K. Knorr, J. Daubert, W. Dultz, and W. J. Fitzgerald. 1980. "Inelastic neutron scattering by coupled rotational and translational modes in KCN." *Zeitschrift für Physik B Condensed Matter* 38 (2): 153–63. https://doi.org/10.1007/bf01598756.



# Inelastic Neutron Scattering by Coupled Rotational and Translational Modes in KCN

A. Loidl* and K. Knorr*
Institut für Physik, Universität Mainz, Mainz, W.-Germany

J. Daubert
Physik Department der Technischen Universität München, Garching, W.-Germany

W. Dultz
Fachbereich Physik der Universität, Regensburg, W.-Germany

W.J. Fitzgerald**
Institut Laue-Langevin, Grenoble, France

The TA [100] phonon branch of the molecular crystal KCN was studied by inelastic neutron scattering in the cubic phase. In addition the distribution of the quasielastic scattered neutrons was investigated. The results are analysed by assuming a coupling of the phonon modes to the rotational degrees of freedom of the CN-dumb-bells which are regarded as a system of interacting quadrupoles. A good description of the present results and also of the existing ultrasonic and Brillouin data is achieved by a simple model which uses a single collective rotational mode of finite excitation energy and line width.

## 1. Introduction

KCN is a molecular crystal with a pseudocubic (NaCl) structure in the high temperature phase. The orientation of the CN-molecules is described by a temperature dependent probability distribution which, at room temperature, shows maxima along the $\langle 111 \rangle$ and minima along the $\langle 110 \rangle$ directions [1]. At 168 K potassium cyanide transforms discontinuously into an orthorhombic structure. The molecules are now aligned in a direction which is closely related to the former cubic [110] axis, but they are still disordered with respect to head and tail [2, 3]. Drastic changes of the orientational distribution just above the phase transition were not observed.

The lattice dynamics of KCN displays some interesting features. Though the estimates for the frequencies of the lowest rotational excitations of the CN-molecules based on thermodynamic and optical measurements are somewhat contradictory, all investigators agree that these excitations should overlap with the translational (or phonon) modes [3–5]. Ultrasonic measurements by Haussühl [6] showed that the elastic constant $c_{44}$ and to a lesser degree also $c'' = (c_{11} - c_{12})/2$ soften towards the phase transition. Analogous results were obtained by Brillouin scattering experiments [7]. Further Brillouin scattering investigations [8] showed that the temperature where the extrapolated data on $c_{44}$ would vanish is independent of pressure whereas the actual transition temperature is not.

In the last couple of years inelastic neutron scattering experiments were performed in the cubic phase of KCN by Rowe et al. [9] and by Daubert et al. [10]. Only a limited number of acoustic phonons could be measured. No defined molecular excitation was observed. The phonon frequency distribution of the high temperature phase is a broad distribution without any marked structure [11]. The phonon dispersion of potassium cyanide at room temperature is quite well described by a harmonic theory [12].

* Research supported by the BMFT, W.-Germany
** Now at Trinity College, Dublin, Ireland

However, this theory fails to explain the low value of the elastic constant $c_{44}$. Recently Rowe et al. [13] explained the line shapes of TA [100] phonons at wavevectors $q/q_{ZB}=0.1$ and 0.5 observed by inelastic neutron scattering by the theory of Michel and coworkers [13, 14] in the limits of a relaxational coupling of the acoustic phonons to reorientational motions of the CN-molecules. Using this interaction in connection with a shell model the anomalous dispersion of the TA phonon branches at room temperature could be reproduced [15]. In this article we will report complete and detailed experimental data of inelastic neutron scattering experiments on the [100] TA branch. In addition we show some results from quasielastic neutron scattering measurements. The results are analysed in terms of a theory of linearly coupled rotational and translational modes. In an extension to the work of Rowe et al. [13] we will present strong evidence that it is necessary to consider molecular excitations at finite energy.

## 2. Theory

The formalism which will be used to analyse the dynamical properties of KCN is based on the theory of Fulde and coworkers [16] which was originally meant to describe the magnetoelastic coupling in the rare earth systems with crystal field split $4f$-states. In the present article it is assumed that this theory on the interaction of phonons with internal electronic degrees of freedom can be applied to KCN where translational modes interact with molecular excitations described by hindered rotations in a Devonshire potential [17]. The advantage of this theory compared to relaxational approaches [13, 18–21] and coupled mode pictures [22–25] is that it imposes no restrictions on the spectrum of the internal excitations, it includes an effective coupling between the internal modes and it includes life time effects. It will be demonstrated that purely relaxational and simple mixed mode models are obtained as limiting cases. The microscopic theory of Michel et al. [14] on the dynamics of molecular crystals with explicit reference to KCN would have been the most appropriate base for the interpretation of the present results, but unfortunately it was worked out in full detail only for the relaxational type of coupling, though in principle the dynamic equations include finite rotational excitations, too.

Starting point of the formalism we use is the dynamic single ion susceptibility of Ref. 16. The crystal field states have to be identified with the eigenstates of the CN-molecule which experiences a single ion Hamiltonian consisting of a free rotator term and the crystal field (Devonshire) potentional of cubic symmetry [17]. Transitions between these states in KCN are called rotational, librational or tunneling transitions depending on the actual change of the wave functions. Each excitation is also characterized by a line width due to damping effects. The term "relaxational transition" might be used in cases where the line width is larger than the energy transfer involved. The mode strength of the excitations is determined by the product of the difference of the thermal population of the two states involved and by the quadrupolar transition matrix elements. In the presence of an effective coupling between the CN-dumb-bells the single ion susceptibility is renormalized. For KCN the coupling has to be regarded as an interaction between the CN-electric quadrupoles which may either be direct or indirect, e.g. mediated by the lattice strains.

In the analysis of the dynamics of KCN the molecular system as described above is linearly coupled to the translational modes. For a translational branch of given symmetry the anharmonic phonon propagator can be written as

$$D^0(\mathbf{q},\omega)=\frac{2\omega_0(\mathbf{q})}{\omega_0^2(\mathbf{q})-\omega^2+2\omega_0(\mathbf{q})\,\pi(\mathbf{q},\omega)} \tag{1}$$

and the phonon self energy $\pi(\mathbf{q},\omega)$ is determined by [26]

$$\pi(\mathbf{q},\omega)=\frac{k_BT}{2v_a}\bar{\gamma}^2\frac{\omega_0(\mathbf{q})}{c_0}\frac{\omega}{\omega+2i\lambda} \tag{2}$$

where $\bar{\gamma}$ is an averaged Grueneisenparameter, $\lambda$ is the inverse average lifetime of thermal phonons and $c_0$ is the elastic constant. This form of the selfenergy is derived by calculating three phonon processes in the high temperature limit ($T>T_{\text{Debye}}$).

In the presence of the coupled molecular excitations the full phonon propagator is now determined by [16]

$$\tilde{D}(\mathbf{q},\omega)=\frac{2\omega_0(\mathbf{q})}{\omega_0^2(\mathbf{q})-\omega^2+2\omega_0(\mathbf{q})\,\pi(\mathbf{q},\omega)-2A^2\omega_0^2(\mathbf{q})\,X(\mathbf{q},\omega)} \tag{3}$$

with $A^2$ being the coupling constant. Note that $\hbar A^2$ is given in terms of an energy and that it is independent of $\mathbf{q}$ and $\omega$. $X(\mathbf{q},\omega)$ is the full susceptibility of the internal modes. Within RPA-MF one obtains [16]

$$X(\mathbf{q},\omega)=\frac{g(\omega)}{1-J(\mathbf{q})\cdot g(\omega)} \tag{4}$$

where $J(\mathbf{q})$ is thought to be an effective coupling, $g(\omega)$ is the single ion susceptibility determined by [16]

$$g(\omega)=-\sum_{ij}\frac{\tilde{O}_{ij}^2(\rho_j-\rho_i)(E_j-E_i)}{\omega^2-(E_j-E_i)^2+i\Gamma\omega}. \tag{5}$$

The $\tilde{O}_{ij}$ are matrix elements describing the transitions between rotator levels and determine the strength of the transitions. $E_i$ is the energy of level $i$, $\Gamma$ an average line broadening and $\rho_i$ the thermal occupation number of the rotator state $i$ divided by the partition function. The symmetry of the phonon branch to which the molecular excitations couple has to be envoked in order to select the appropiate matrix elements. In the case of an interaction with the acoustic branches with sound velocities proportional to $c_{44}^{1/2}$ or $\left(\frac{c_{11}-c_{12}}{2}\right)^{1/2}$ the matrix elements are of quadrupolar type and transform according to the $T_{2g}$ and $E_g$ irreducible representations of the cubic group.

Using magnetic analogies contributions coming from transitions with $i\neq j$ are called Van Vleck terms. Further contributions arise from terms where $i=j$. Using

$$\lim_{|E_i-E_j|\to 0}\frac{\rho_j-\rho_i}{E_j-E_i}=\frac{\rho_i}{k_BT}$$

these terms are identified as the Curie contributions to the static susceptibility $g(0)$.

Assuming the simplest case of a singlet-singlet system with a level separation of $\Delta=|E_1-E_2|$ the single ion susceptibility contains a single Van Vleck term, which in the high temperature limit ($\hbar\Delta\ll k_BT$) has the form

$$g(\omega)=-\frac{\hbar\tilde{O}^2}{2k_BT}\frac{\Delta^2}{\omega^2-\Delta^2+i\Gamma\omega}. \tag{6}$$

In the limit of $\omega\ll\Delta$ this further reduces to

$$g(\omega)\sim\frac{1}{T}\frac{1}{1-i\omega\tau} \tag{7}$$

with a relaxational time $\tau=\Gamma/\Delta^2$ which is the ansatz for the purely relaxational 'spin'-phonon system used by several authors [18–21]. In the case of a singlet-singlet system with $\Gamma\ll\Delta$, i.e. with a single well defined rotational transition, the poles of the phonon propagator of (3) yield a simple mixed mode excitation spectrum of the coupled rotational and translational modes. Assuming that the coupling $J(\mathbf{q})$ between the CN-dumb-bells extends to the next nearest neighbours only, it is given in the $fcc$-type structure of KCN by

$$\begin{aligned}J(\mathbf{q})=\frac{J_0}{6}\Big\{&\cos\frac{\pi}{2}(q_x+q_y)+\cos\frac{\pi}{2}(q_x-q_y)\\&+\cos\frac{\pi}{2}(q_x+q_z)+\cos\frac{\pi}{2}(q_x-q_z)\\&+\cos\frac{\pi}{2}(q_y+q_z)+\cos\frac{\pi}{2}(q_y-q_z)\Big\}\end{aligned} \tag{8}$$

The excitation spectrum $\omega_R(\mathbf{q})$ of the rotational modes is determined by the poles of (4). If we restrict $g(\omega)$ to a singlet-singlet system and if damping effects are small the poles of $X(\mathbf{q},\omega)$ are determined from

$$1+J(\mathbf{q})\frac{\hbar}{2k_BT}\frac{\tilde{O}^2\Delta^2}{\omega^2-\Delta^2}=0 \tag{9}$$

which yields

$$\omega_R(\mathbf{q})=\Delta\left[1-\frac{\hbar\tilde{O}^2}{2k_BT}\cdot J(\mathbf{q})\right]^{1/2} \tag{10}$$

In the long wavelength limit $\mathbf{q}\to 0$ the static susceptibility gives

$$\chi(0,0)=\frac{g(0)}{1-J_0g(0)} \tag{11}$$

with $g(0)$ as deduced from (6), namely

$$g(0)=\frac{\hbar\tilde{O}^2}{2k_BT}. \tag{12}$$

The poles of $\chi(0,0)$ determine the 'Curie'-temperature $T_C$ where the CN-dumb-bells achieve quadrupolar order, with

$$T_C=J_0\cdot\frac{\hbar\tilde{O}^2}{2k_B} \tag{13}$$

Finally the poles of $\tilde{D}(\mathbf{q},\omega)$ (Eq.(3)) describe the excitations of the system. They are given by

$$\begin{aligned}\omega^2=&\omega_0^2(\mathbf{q})+2\omega_0(\mathbf{q})\cdot\pi(q,\omega)\\&-2A^2\omega_0^2(\mathbf{q})X(\mathbf{q},\omega).\end{aligned} \tag{14}$$

In the limit $\mathbf{q}\to 0$ one obtains $\omega=v\cdot|\mathbf{q}|$ and $\omega_0=v_0|\mathbf{q}|$. These equations allow us to determine the temperature dependence of the sound velocity $v$ or of the appropiate elastic constants in the presence of rotational-translational interactions. By dividing (14) by $q^2$ and taking the limits $q\to 0$ and $\omega\to 0$ one finds [16]

$$v^2=v_0^2[1-2A^2\cdot X(0,0)]. \tag{15}$$

It is obvious that the renormalized sound velocity softens with falling temperature because of the

growth of the static bulk susceptibility $X(0, 0)$. Eventually, at a characteristic temperature $T_S$, $v$ will vanish. $T_S$ is understood as the transition temperature if the structural phase transition were strictly of second order. Rewriting $X(0,0)$ as a Curie-Weiss-law using the definition of $T_C$ (Eq. (13)), $T_S$ is obtained from the root of (15) as

$$(T_S - T_C) = \frac{\hbar}{k_B} \cdot A^2 \cdot \tilde{O}^2. \tag{16}$$

Reinserting this result in (15) gives the wellknown form of the temperature dependence of the elastic constants

$$c = c_0 \frac{T - T_S}{T - T_C} \tag{17}$$

where $T_C$ and $T_S$ are determined by (13) and (16) respectively.

Finally in an inelastic neutron scattering experiment the differential cross section is determined by

$$\frac{d^2\sigma}{d\Omega\, d\omega} = \frac{k_f}{k_i} S(\mathbf{Q}, \omega). \tag{18}$$

The dynamic structure factor can be written as

$$S(\mathbf{Q}, \omega) \sim (n(\omega) + \tfrac{1}{2} \pm \tfrac{1}{2}) \operatorname{Im} \mathbf{D}(\mathbf{q}, \omega) \tag{19}$$

where the positive sign stands for neutron energy loss and the negative sign for neutron energy gain. The formalism outlined above assumes explicitely that the molecular excitations are seen only indirectly in a neutron scattering experiment by their admixture to the phonon states. Of course, these excitations could also be probed directly by neutron scattering since they involve the motion of the $C$ and $N$ scattering centers. Sufficiently high scattering intensity for this direct process is however only expected at $\mathbf{Q}$-vectors which correspond to the maxima of the molecular form factor.

For the momentum transfers used in the present experiment the indirect process should give the higher scattered intensities, though admixtures from the direct process cannot be ruled out completely.

## 3. Experiments and Results

The single crystal of KCN was grown from solution and had a size of $2\,\mathrm{cm}^3$ with a mosaic spread of less than 0.3°, although a Bragg tail was detectable far out in the Brillouin zone. The measurements were performed on the triple-axis spectrometer IN2, situated at the thermal neutron beam tube of the HFR at the ILL Grenoble. Incident wave vectors $k_i = 2.662\,\text{Å}^{-1}$ and $1.55\,\text{Å}^{-1}$ were used with a pyrolytic graphite double-monochromator and a graphite analyser. Higher order contaminations were reduced using a pyrolytic graphite filter at the higher energy and a cooled Beryllium filter at the lower energy. A horizontal collimation with $120' - 30' - 30' - 30'$ was used throughout the measurements. The energy resolution (FWHM) as determined by incoherent scattering of a vanadium standard was 220 GHz at $k_i = 2.662\,\text{Å}^{-1}$ and 28 GHz at $1.55\,\text{Å}^{-1}$. The constant $-\mathbf{Q}$ and the constant-$E$ mode of operation were used in this experiment with $k_i$ kept constant for all the scans. For reduced phonon wave vectors $q/q_{ZB} \leqq 0.25$ the lower incident energy was used, while the rest of the scans was performed at the higher energy. The experiments were carried out in the (001)-plane as well as in the $(01\bar{1})$-plane of the crystal.

In order to convert the raw data of neutron counting rates $I(\mathbf{Q}, \omega)$ at a given point of the $(\mathbf{Q}, \omega)$-space into the dynamic structure factor $S(\mathbf{Q}, \omega)$ the spectrometer efficiency has been considered. Assuming that the dispersion relation is planar the detector counting rate for constant monitor count is [27]

$$I(\mathbf{Q}, \omega) = A_0 \frac{k_f}{k_i} \frac{\varepsilon_D}{\varepsilon_M} \operatorname{ctg} \Theta_A R_A k_f^2 S(\mathbf{Q}, \omega) + B \tag{20}$$

where $A_0$ is a scale factor, $\Theta_A$ and $R_A$ are the Bragg angle and reflectivity of the analyser, $\varepsilon_D$ and $\varepsilon_M$ are the efficiencies of the detector and monitor. $B$ is the background counting rate. Figure 1 shows equal intensity contour maps in the [100]-direction with transverse polarisation just above the phase transition. The data with lower and higher incident energies are plotted separately. The scattered neutron intensities have been corrected using (20) to yield the dynamic structure factor $S(\mathbf{Q}, \omega)$. Clearly the data fail to show any pronounced peaked structure in reduced wave vector range $0.15 < q/q_{ZB} < 0.8$. In this region one finds weak defined shoulders on an intensity profile which increases monotonically towards $\omega = 0$. At small phonon wave vectors the sacttered neutron intensities show distinct one phonon excitations. The centers of these peaks coincide well with the extrapolated ultrasonic data [6] (dashed line in the figure). Near the zone boundary weak but defined peaks are observed. There is a weak but significant additional structure in the wings of the contour lines in the energy range around 1 THz and which fills the gap between the phonon signal and the peak at zero energy transfer. The hybridisation of the transverse acoustic mode with a heavily damped rotational

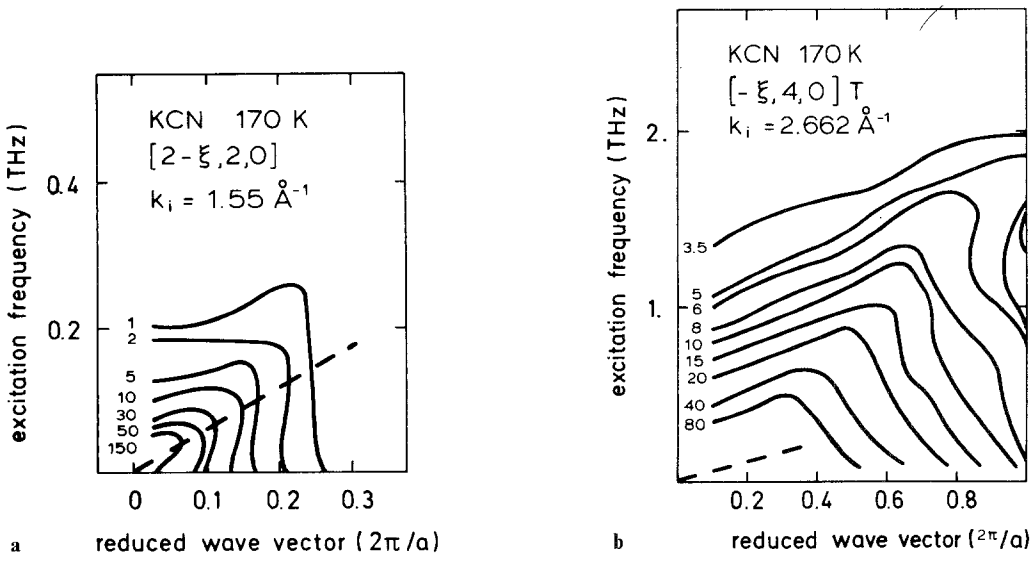


**Fig. 1 a and b.** Equal intensity contour maps along[100]T at 170 K. The data were collected utilizing incident wave vectors of $k_i = 1.55$ Å$^{-1}$ **a** and $k_i = 2.662$ Å$^{-1}$ **b**. The raw data were corrected to yield the dynamic structure factor. The dashed lines indicate the extrapolated ultrasonic data of the elastic constant $c_{44}$

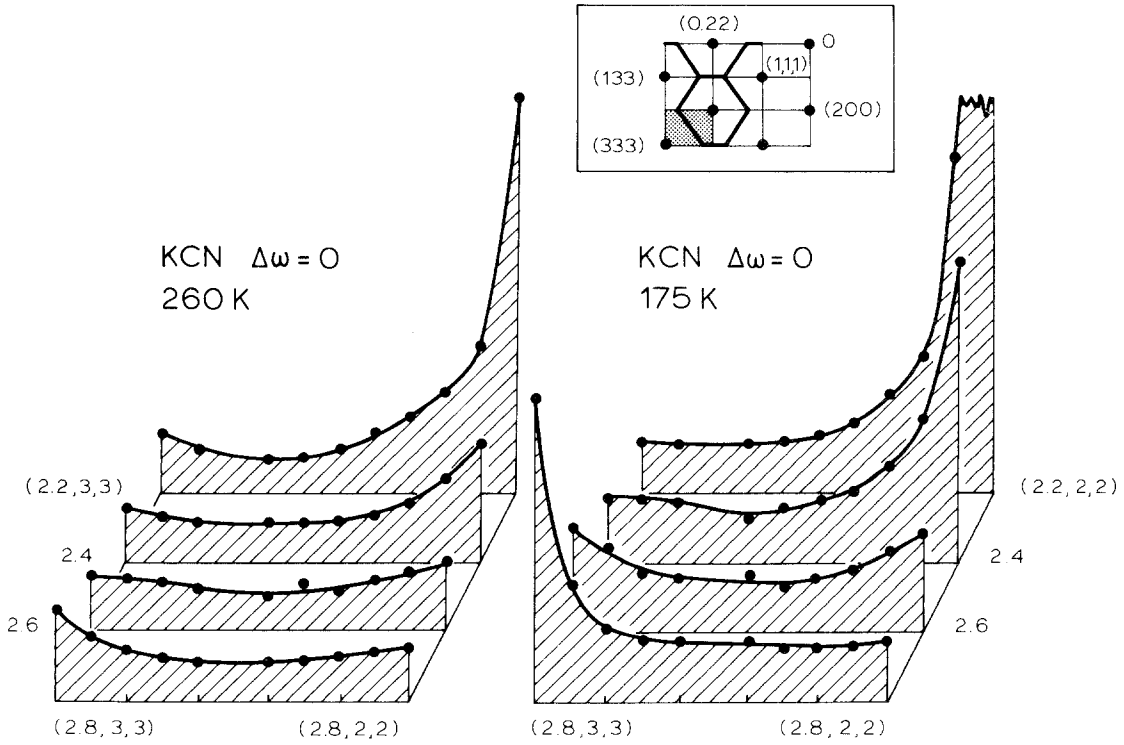


**Fig. 2.** Intensity from constant-$E$ scans with zero-energy transfer at 175 K and at 260 K. The lines serve as a guide to the eye. The inset shows the reciprocal lattice and the Brillouin zones of the $fcc$ lattice. The shaded area indicates the region where the scans were performed

mode can account for this effect, and will be qualitatively explained in the next chapter. Figures 2 and 3 show some scans which were performed to determine the diffuse scattered intensities in the (01$\bar{1}$)-plane. These data were obtained with an incident wavevector $k_i = 2.662$ Å$^{-1}$ and at zero-energy transfers. One clearly observes that there is modulation of the quasielastic scattered intensities in **Q**-space which is strongly temperature dependent. In Fig. 2 maximum counting rates appear along [$\zeta$00]T growing to-

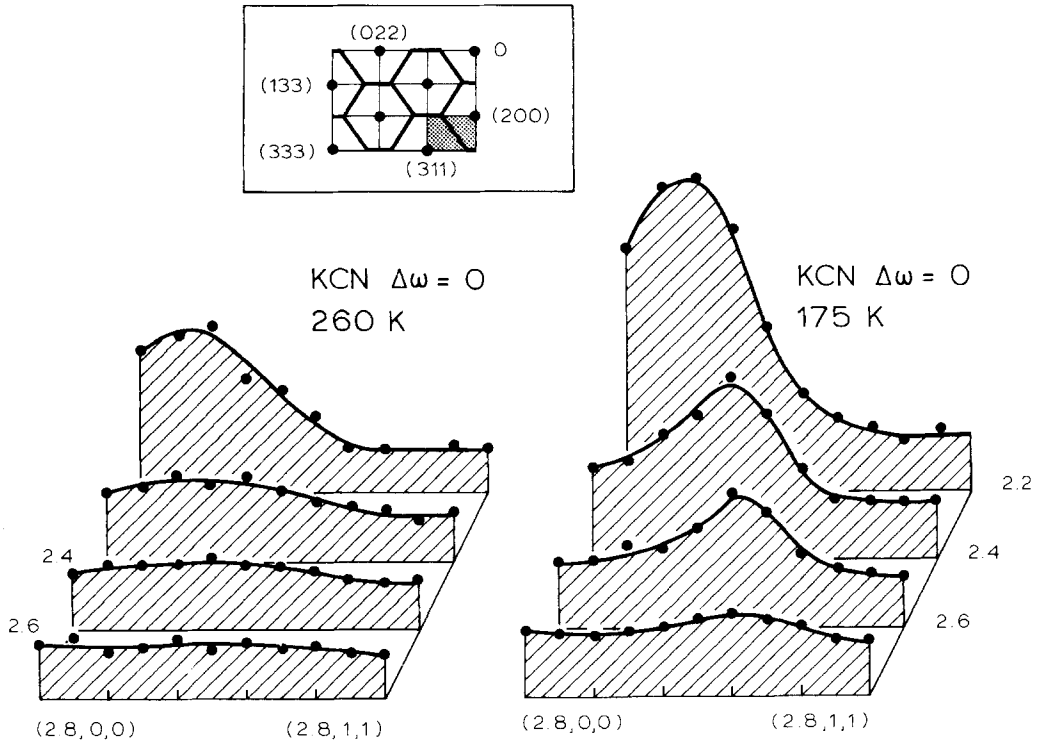


**Fig. 3.** Intensity from constant-$E$ scans at zero-energy transfer at 175 K and 260 K. The lines are drawn to guide the eye. The shaded area in the inset shows the corresponding region in reciprocal space

wards the Bragg points (222) and (333), which increase when approaching the phase transition. These intensities along $[\zeta 00]$, which can also be seen in Fig. 1, originate from the coupling of the transverse acoustic mode and the rotational excitations of the CN-dumb-bells with $T_{2g}$ symmetry. Similar structures are obtained in the $[0\zeta\zeta]$ directions and in the (001) plane in $[\zeta 00]$ directions.

An interesting feature are the quasielastic scattered intensities along $[\zeta\zeta\zeta]$ as shown in Fig. 3. These extra intensities are increasing towards the (002) bragg reflection and develop continuously through the zone boundary. There is no increase towards the (311) bragg peak. These findings have also been veryfied around the (022) and (222) lattice points. The pattern of these diffuse scattered intensities exclude the possibility, that they originate in the coupling of rotational and translational modes of different symmetry. Static correlations of the CN-dumb-bells can account for it and quantitative calculations are in progress.

## 4. Analysis of the Experimental Data

The aim of this chapter is to calculate some dynamic and static properties of KCN using the model outlined in § 2 and compare it to the experimental results. To do so we must make some assumptions concerning the molecular susceptibility. Unfortunately, the exact scheme of the single ion states of the CN-ion in KCN is still unknown. From the theoretical calculations [17] it is expected that a large number of states are populated in the temperature region of the present study and that several transitions among these states are possible even if quadrupolar transitions of $T_{2g}$ symmetry are considered only. Qualitatively speaking it is probably justified to assume a tunnel split ground state centered along the $\langle 111 \rangle$ directions followed by low lying rotational states which describe the oscillations of the molecules in the hindering wells of the Devonshire potential. In order to allow for transitions of finite energy transfer and also to keep the number of free parameters small we use the simplest model possible for this case: The singlet-singlet model, which was already extensively described in the theoretical part of this article. We suppose that this model is more realistic than the purely relaxational approach of Ref. 13, since there is a mixing of translational and rotational modes at finite energies as demonstrated in Fig. 1. Furthermore, rotational transitions in the frequency range of 0.5 to 1 THz were observed in the mixed crystals $KCl_{1-x}CN_x$ [24], $KBr_{1-x}CN_x$ [28] and CsCN [29].

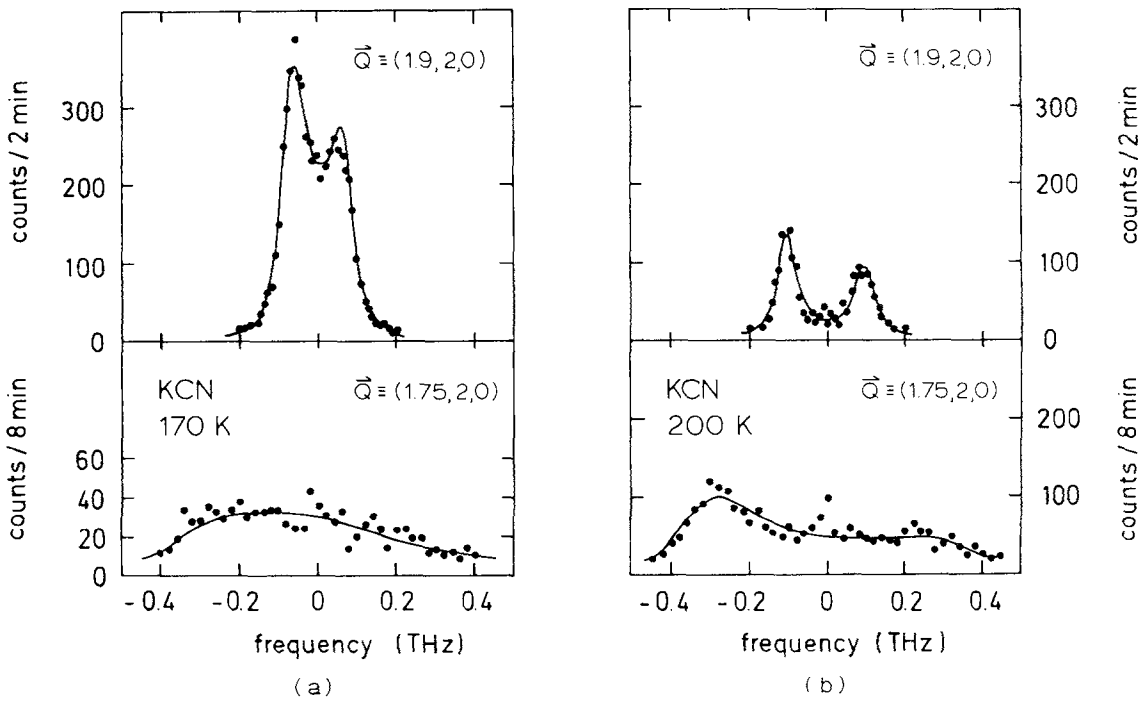


**Fig. 4a and b.** Neutron line shapes collected with incident neutron wave vector $k_i = 1.55\,\text{Å}^{-1}$ at 170 K **a** and at 200 K **b**. The lines are fits of the theoretical model to the experimental data

*4.1. Inelastic Neutron Scattering*

To be specific, in the model used to fit the neutron line shapes the single ion susceptibility of (6), the full susceptibility of (4) in connection with the 'exchange' coupling of (8) were considered. The dynamic structure factor $S(\mathbf{Q}, \omega)$ was finally calculated from (2), (3) and (19). The dispersion of the bare phonon frequencies $\omega_0(\mathbf{q})$ was simply assumed to follow a sinusoidal dependence with the initial slope determined by the background elastic constant $c_{44}^0$. The relevant parameters are $c_{44}^0$, the level spacing $\Delta$, the line broadening $\Gamma$ of the rotational excitation, the average Grueneisenparameter $\bar{\gamma}$, the phonon damping $\lambda$, and the two characteristic temperatures $T_c$ and $T_s$.

The result in the fitting is shown in Figs. 4 and 5. The presentation in terms of constant-**Q** scans rather than in terms of a contour plot was chosen for better clarity. Each constant-**Q** scan was fitted by a separate set of parameters. One notes that the agreement between theory and experiment is very good. Table 1 gives the mean parameters of all scans and the maximum variations from the average values. Due to the relatively small variations the overall fit for all **Q**-values using the mean parameters is only slightly worse. In the temperature range investigated no significant change of the parameters was detected. The three parameters $T_c$, $\Delta$ and $\Gamma$ characterize the $CN^-$-system. The rotational excitation energy $\Delta$ is about 1.5 THz. From the approximate, though incomplete knowledge of the single ion states of CN in KCN one might assume that this excitation is the transition from the ground state to the first excited librational state with both states centered along the $\langle 111 \rangle$ wells of the Devonshire potential. This situation corresponds to crystal field parameters of about $\phi = 240°$, $K = -30$ and $B = 0.05$ THz in the nomenclature of Beyerle [17], where $B$ is the rotational constant, $K$ measures the intensity of the potential and $\phi$ determines its shape. The finite lifetime $\Gamma$ might be a genuine lifetime effect, but also could include the splitting of the ground state and in particular of the first excited state due to the finite height of the potential barriers separation in the eight $\langle 111 \rangle$ wells. The effective coupling of the CN-molecules which is described by the quadrupolar ordering temperature $T_C$ is of relatively little importance. The coupling is thought to be mediated by local strains round the CN-dumb-bells [14, 31]. Just above the structural phase transition at 168 K the propagating rotational excitation has only developed a bandwidth of 0.3 THz as calculated according to (17), with a minimum excitation energy at the $\Gamma$-point due to the ferrodistortive character of the interaction. Quadrupolar order of the CN-dumb-bells in the cubic phase would be approached at 50 K. The three parameters $c_0$, $\bar{\gamma}$ and $\lambda$ characterize the phonons decoupled from the internal excitations. Their values are comparable

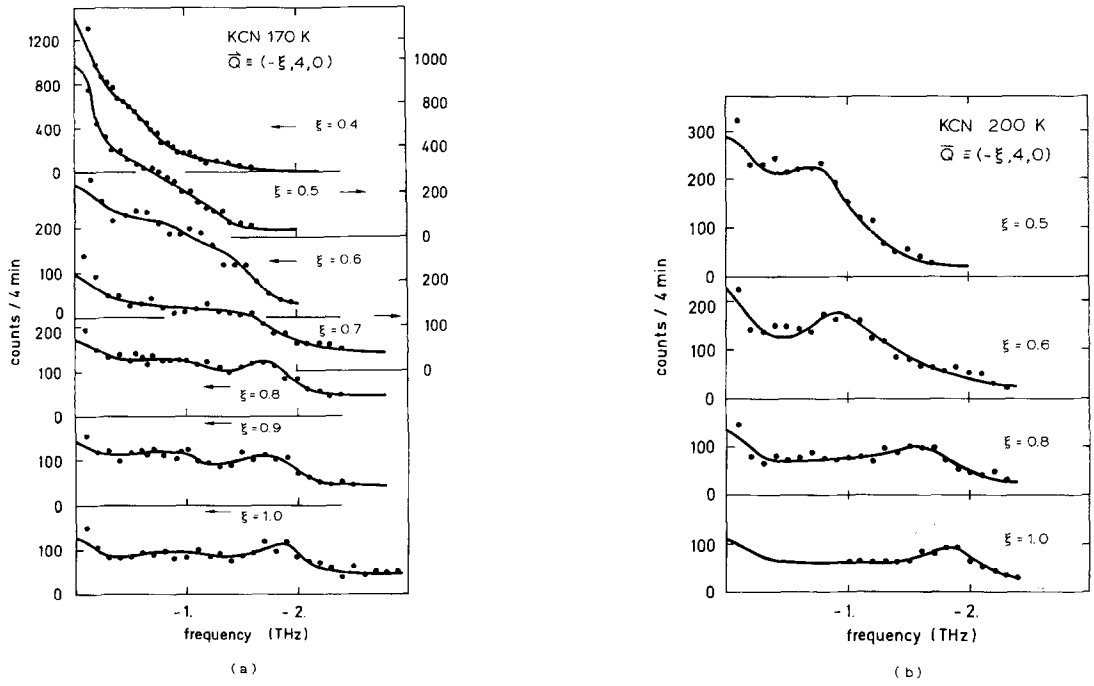


**Fig. 5a and b.** Neutron line shapes collected with $k_i = 2.662\,\text{Å}^{-1}$ at 170 K **a** and at 200 K **b**. The lines represent the result of the theoretical model to the experimental data

**Table 1.** Parameters of a singlet-singlet model fitted to the observed neutron line shapes at two temperatures

| Parameter (units) | 170 K | 200 K |
|---|---|---|
| $T_C$ (K) | 49 ±15 | 42 ±10 |
| $T_S$ (K) | 150 ±15 | 152 ±12 |
| $c_0$ ($10^{10}$ dyn/cm$^2$) | 3.6± 0.4 | 3.7± 0.2 |
| $\Delta$ (THz) | 1.5± 0.2 | 1.6± 0.2 |
| $\Gamma$ (THz) | 1.4± 0.2 | 1.6± 0.3 |
| $\bar{\gamma}$ | 1.3± 0.2 | 1.6± 0.2 |
| $\lambda$ (THz) | 0.2±0.1 | 0.25± 0.1 |

to those observed in KBr. At room temperature the corresponding values in KBr are $c_0 = 5.07$ [32] and the mean Grueneisenparameter $\bar{\gamma}$ is equal to 1.5 as cited after Cowley and Cowley [33]. The values of calculated phonon halfwidths of optic modes in KBr are in the order of 0.1 THz [33]. Finally, $T_S - T_C$ is a measure of the 'spin'-lattice coupling. Not surprisingly, the coupling in KCN exceeds by order of magnitude the coupling in real spin systems, it is of the same order as the other characteristic frequencies occuring in this molecular crystal, a fact which can be supposed from realizing simply the interionic distances and ionic masses in potassium cyanide.

The pattern of scattered intensities at different values of $q/q_{ZB}$ is due to a delicate balance of the characteristic energies $\Delta$, $\gamma$, $\omega_0$ and the $q$-dependent coupling $(A^2\omega_0^2)$. There are three $q$-ranges of basically different behaviour: For large reduced wave vectors near the zone boundary, $q/q_{ZB} \geqq 0.8$, the decoupled phonon frequency is larger than the line width of the rotational transition and the characteristic two peak structure of a coupled mode picture is obtained, although the rotational mode is heaviliy damped. An additional central peak due to a decay of the coupled modes into a relaxational channel is observed. It is this range which could not be described by the purely relaxational approach. At intermediate $q$-values $0.3 \leqq q/q_{ZB} \leqq 0.7$ the phonon frequencies are of the order of the line-broadening $\Gamma$ and give rise to a quasielastic continuum of almost Lorentzian line shape. At low $q$'s, $q/q_{ZB} < 0.3$, the phonon recovers as well defined excitation from the quasielastic continuum because $\omega_0$ is now much smaller than $\Gamma$. These three regions correspond to the cases of slow, intermediate and fast relaxation of the pseudospin model of Yamada et al. [19]. Because of the temperature dependence of the coupling between spin and phonons the spectra at 200 K show slightly better defined translational excitations.

### *4.2. Quasielastic Neutron Scattering*

In the framework of this model it is also possible to calculate the quasielastic neutron intensities which originate in the coupling of the rotational excitations to translational modes by taking the limit $\omega \to 0$ of the dynamic structure factor $S(\mathbf{q}, \omega)$. For different

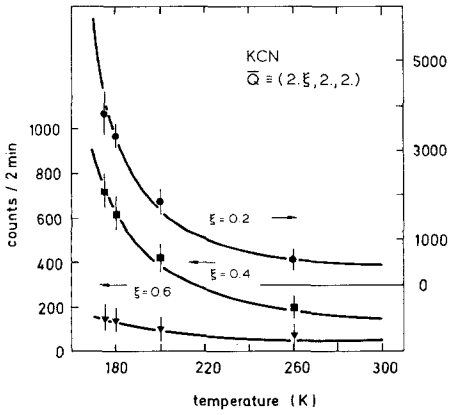


**Fig. 6.** Temperature dependence of intensities at zero-energy transfer along [100] T at different phonon wave vectors. The full lines are the result of the theoretical model, with the scale factor as the only free parameter. The incoherent elastic scattering is substracted

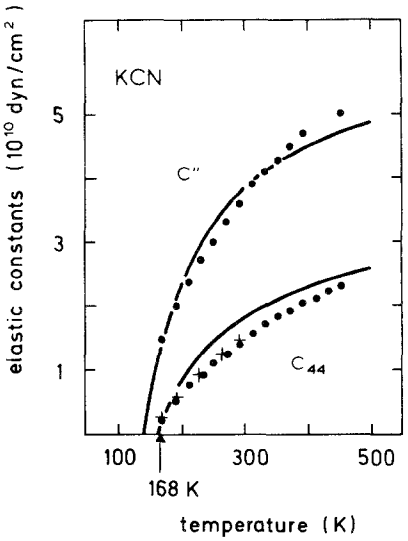


**Fig. 7.** Temperature dependence of the elastic constants $c_{44}$ and $c'' = (c_{11} - c_{12})/2$. The experimental data from ultrasonic (●) [6] and Brillouin measurements (+) [7] are compared to the theoretical results. Note that the temperature dependence of $c_{44}$ is calculated with no free parameter. In the case of $c''$, $T_S$ and $(c'')^0$ are the parameters varied

phonon wavevectors and temperatures these results are compared with the experimental data in Fig. 6. Theory and experiment coincide within the experimental errors. For the calculations the averaged parameters at 170 K and 200 K of Table 1 were used. The **q**-dependent modulation of the quasi-elastic intensities which has the shape of a ridge along the [100] direction as shown in Fig. 2 is well understood by taking account of polarisation effects and of the wave vector dependence of the appropriate elastic constants.

### *4.3. Ultrasonic and Brillouin Results*

The temperature dependence of the elastic constants of KCN has been investigated by ultrasonic [6] and Brillouin [7] measurements. The results on $c_{44}$ and $c'' = (c_{11} - c_{12})/2$ are reproduced in Fig. 7, where the predictions of the present model using (16) are shown as solid lines. For the calculations of $c_{44}(T)$ the values of $T_C$, $T_S$ and $c_{44}^0$ as derived from the fit to the long wave length neutron data ($q/q_{ZB} \leqq 0.25$) only were used, namely $T_C = 40$ K, $T_S = 152$ K and $c_0 = 3.5\ 10^{10}$ dyn/cm$^2$. The theoretical curve for $c''(T)$ is the best fit to the experimental data with the free parameters $T_S''$ and $c''^0$ which adopted the values 139 K and $6.2 \cdot 10^{10}$ dyn/cm$^2$. $T_C$ was held constant at the value of 40 K since the same Curie temperature must govern the softening of all strains. One notes that the experimental result is fairly well reproduced by the present model. A fit to the results of Ref. 6 with all parameters freely varying was carried out by Rehwald et al. [31]. One finds that the most significant differences appear in $T_C$ where Rehwald's data ($T_C = -231$ K) suggest an 'antiferrodistortive' ordering of the CN-dumb-bells, i.e. a softening of rotational modes at the zone boundary, while our data yield a softening at the zone center.

The results of Fig. 7 clearly demonstrate that the stability limits of the high temperature phase as given by the temperatures $T_S$ are very close together. This behaviour elucidates the fact that only the coupling of both strains to rotational states can explain the reduction of symmetry at the 168 K phase transition in KCN [30, 31].

We think that an interpretation of the Brillouin data on the pressure dependence of sound waves in KCN [8] is not meaningful since practically all parameters involved in the present model are susceptible to pressure, namely the level spacing, the transition matrix elements, the exchange coupling and the coupling of translational modes with molecular excitations. With the present knowledge of KCN a theoretical treatment of the pressure dependence of $T_S$ is impossible. As the phase transition is of first order the calculation of the actual transition temperature is even more complicated. The pressure dependence of these two parameters yields no straight forward information on the nature of the phase transition in potassium cyanide.

Recent results on the Brillouin linewidths of phonons in KCN [34] can be easily explained within the model proposed above. The damping of phonons coupled to the pseudospin system is determined by the imaginary part of (14). Assuming the limits $\omega \ll \Delta$ and $q/q_{ZB} \ll 2\pi/a$, which hold for Brillouin experi-

ments, it is straightforward to find the damping of transverse phonons $\Lambda_{TA}$ in the high temperature limit, namely

$$\Lambda_{TA}(\omega)=\Lambda_1^0(\omega)\cdot T+\Lambda_2^0(\omega)\frac{T}{(T-T_C)^2} \tag{21}$$

where the first term is the usual damping resulting from three-phonon collisions, while the second term is an additional linewidth due to the coupling of the translational modes to the interacting *CN*-dumb-bells. $\Lambda_1^0$ and $\Lambda_2^0$ are purely frequency dependent factors.

Experimentally, a decrease of the linewidth with increasing temperature was observed from about 20 MHz at 170 K to approximately 10 MHz at 300 K for TA [100] phonons. Neglecting the phonon term which is small for temperatures below 300 K one finds theoretically a decrease by a factor of 2.3 in the same temperature interval.

## 5. Conclusions

In the present investigation detailed results of inelastic and quasielastic neutron scattering experiments in potassium cyanide are presented. These data yield strong evidence for the coupling of rotational and translational modes in KCN, where the rotational excitations appear at finite energy transfers of the order of 1.5 THz. These experimental findings are described as a coupled phonon-rotational excitation system. The molecular susceptibility was approximated by a single Van Vleck term including a line broadening and by assuming an effective exchange coupling between the CN-dumb-bells to the next nearest neighbours only. All information available on the dynamic properties of the system, ultrasonic, Brillouin and neutron data could be reasonably fitted by a single set of parameters with this model, although the actual scheme of the rotational excitations of the CN-molecules in KCN is certainly more complex. The distribution of inelastic scattered neutron intensities along [100] T showed three characteristic ranges depending on the balance of the linewidth of the rotational modes and the decoupled phonon energy. The softening of the translational modes can be easily understood with this simple and comprehensive picture. The phase transition in potassium cyanide at 168 K occurs because of the bilinear coupling between rotational and translational modes of $E_g$ and $T_{2g}$ symmetry and, as stated previously in Refs. 13 and 31, should be thought of as being analogous to that in cooperative Jahn-Teller systems.

The authors are indebted to Professor S. Haussühl who kindly supplied us with the KCN single crystal.

## 7. References

1. Rowe, J.M., Hinks, D.G., Prince, D.L., Susman, S.: J. Chem. Phys. **58**, 2039 (1973)
   A slightly more sophisticated model, including anisotropic center-of-mass motions yield in the case of KCN very similar results to that obtained by Rowe et al.
   Sievers, U., Loidl, A., Heeger, G. (unpublished)
2. Bijvoet, J.M., Lely, J.A.: Rec. trav. chim. **59**, 908 (1940)
3. Suga, H., Matsuo, T., Seki, S.: Bull. Chem. Soc. Jap. **38**, 1115 (1965)
4. Dultz, W.: Solid State Commun. **15**, 595 (1974)
5. Fontaine, D., Poulet, H.: Phys. Status Solid B **58**, K9 (1973)
6. Haussühl, S.: Solid State Commun. **13**, 147 (1973)
7. Krasser, W., Buchenau, U., Haussühl, S.: Solid State Commun. **18**, 287 (1976)
8. Hochheimer, H.D., Love, W.F., Walker, C.T.: Phys. Rev. Lett. **38**, 832 (1977)
9. Rowe, J.M., Rush, J.J., Vegelatos, N., Prince, D.L., Hinks, D.G., Susman, S.: J. Chem. Phys. **162**, 4551 (1975);
   Rowe, J.M., Rush, J.J., Prince, E., Chesser, N.J.: Ferroelectrics **16**, 107 (1977)
10. Daubert, J., Knorr, K., Dultz, W., Jex, H., Currat, R.: J. Phys. C **9**, L389 (1976)
11. Nücker, N., Knorr, K., Jex, H.: J. Phys. C **11**, 1 (1978)
12. Jex, H., Maetz, C.J.: Phys. Status Solidi B **85**, 511 (1978)
    Bill, C.J., Jex, H., Müllner, M.: Phys. Lett. **56** A, 320 (1976)
13. Rowe, J.M., Rush, J.J., Chesser, N.J., Michel, K.H., Naudts, J.: Phys. Rev. Lett. **40**, 455 (1978)
14. Michel, K.H., Naudts, J.: Phys. Rev. Lett. **39**, 212 (1977); J. Chem. Phys. **67**, 547 (1977); J. Chem. Phys. **68**, 216 (1978)
    Michel, K.H., Naudts, J., De Raedt, B.: Phys. Rev. B **18**, 648 (1978)
15. Strauch, D., Schröder, U., Bauernfeind, W.: Solid State Commun. **30**, 559 (1979)
16. Fulde, P.: Handbook on the Physics and Chemistry of Rare Earths. Gschneidner, K.A., Eyring, L. (eds.), p. 295, Amsterdam: North Holland Pub. 1978
    Fulde, P.: Z. Physik B **20**, 89 (1975);
    Dohm, V., Fulde, P.: Z. Physik B **21**, 369 (1975)
17. Beyeler, H.U.: Phys. Status Solidi B **52**, 419 (1972)
18. Huberman, B.A., Martin, R.M.: Phys. Rev. B **13**, 1498 (1976); Phys. Rev. Lett. **39**, 478 (1977)
19. Yamada, Y., Taktera, H., Huber, D.L.: J. Phys. Soc. Jap. **36**, 641 (1974)
    Yamada, Y.: Ferroelectrics **16**, 49 (1977);
    Yamada, Y., Noda, Y., Axe, J.D., Shirane, G.: Phys. Rev. B **9**, 4429 (1974)
20. Silverman, B.D.: Phys. Rev. Lett. **25**, 107 (1970)
    In this study the spin susceptibility includes a finite tunneling frequency
21. Elliott, R.J., Young, A.P.: Ferroelectrics **7**, 23 (1974)
22. Elliott, R.J., Harley, R.T., Hayes, W., Smith, S.R.P.: Proc. Roy. Soc. Lond. A **328**, 217 (1972)

23. Schober, H.R., Tewary, V.K., Dederichs, P.H.: Z. Physik B**21**, 255 (1975)
24. Wood, R.F., Mostoller, M.: Phys. Rev. Lett. **35**, 45 (1975)
25. Walton, D., Mook, H.A., Nicklow, R.M.: Phys. Rev. Lett. **33**, 412 (1974)
26. Loidl, A.: J. Phys. F**7**, L57 (1977)
27. Chesser, N..J, Axe, J.D.: Acta Crystallogr. A**29**, 160 (1973)
Dorner, B.: Acta Crystallogr. A**28**, 319 (1972)
28. Measurements of coupled modes in $T_{2g}$ symmetry in $KBr_{0.86}CN_{0.14}$ revealed transitions in the order of 1 THz
Loidl, A., Feile, R., Knorr, K., Renker, B., Daubert, J., Durand, D.: (to be published)
29. Loidl, A., Kjems, J., Haussühl, S.: (to be published)
30. By means of group-subgroup relations it was shown that the phase transition in KCN at 168 K consists of two translationally equivalent transitions of index 3 and index 2
Heger, G., Loidl, A.: Progress Report IAK, Kernforschungszentrum Karlsruhe 2670, 41 (1978)
31. Rehwald, W., Sandercock, J.R., Rossinelli, M.: Phys. Status Solidi A**42**, 699 (1977)
32. Haussühl, S.: Z. Physik **159**, 223 (1960)
33. Cowley, E.R., Cowley, R.A.: Proc. Roy. Soc. A**287**, 259 (1965)
34. Boissier, M., Vacher, R., Fountaine, D., Pick, R.M.: Proc. of the Int. Conf. on Lattice Dynamics. Balkanski, M. (ed.) p. 641, Paris: Flammarion 1978

A. Loidl
K. Knorr
Institut für Physik
Johannes Gutenberg-Universität Mainz
Jakob-Welder-Weg 11
D-6500 Mainz
Federal Republic of Germany

J. Daubert
Physik-Department
Technische Universität München
D-8046 Garching bei München
Federal Republic of Germany

W. Dultz
Fachbereich Physik
Universität Regensburg
Universitätsstraße 31
8400 Regensburg
Federal Republic of Germany

W.J. Fitzgerald
Institut Max von Laue-Paul Langevin
156X
F-38042 Grenoble Cedex
France